BNL-64839
CONF-9709124--

NEUTRON SCATTERING INVESTIGATIONS OF THE DYNAMICS OF THIN FILMS ADSORBED ON SOLID SURFACES

J. Z. Larese
Chemistry Dept.
Brookhaven National Laboratory
Upton, NY 11973, USA

While not commonly thought of as surface sensitive probes, high-resolution inelastic and quasielastic neutron scattering (INS) techniques can be used to investigate the dynamical properties of films adsorbed on solid surfaces. These studies are possible because the adsorption takes place on samples which exhibit a large surface-to-volume ratio. By combining dynamical measurements with data from structural, thermodynamic and computer simulation studies it is then possible to develop a comprehensive picture of the microscopic properties of an adsorbed film system. In order to illustrate the power of employing INS techniques we will discuss the continuous melting of monolayer ethylene and the layer-by-layer melting of multilayer argon films on the basal plane of graphite and the rotational tunneling of methane films on the MgO(100) surface.

Introduction

Neutron scattering techniques are used in many areas of condensed matter science because the energies and wavelengths of thermal neutrons cover those length and energy scales associated with the interatomic distances and dynamical response of most materials. It is therefore, not surprising that neutron scattering research has made *fundamental* contributions to a host of scientific disciplines and areas of engineering. Neutrons interact weakly with matter so they have been used less frequently in the field of surface science. By employing materials that are both crystalline and exhibit a large surface-to-volume ratio like exfoliated graphites and MgO powders a wealth of information has been recovered about the structure and dynamics of adsorbed surface films. In this article we will describe how neutron techniques (with an emphasis on dynamical studies) have been used to investigate the melting properties of ethylene on graphite, the layer-by-layer melting of multilayer argon films on graphite and the rotational tunnelling of methane films on MgO(100) surfaces. It is our goal to illustrate the power of using both elastic and inelastic cold neutron techniques in concert with other methods (thermodynamic and computer simulation) to study the structure and dynamics of these overlayer systems.

Ethylene Melting

Ordinary, 3D matter is known to melt at a single point via an abrupt, first-order process. Typical of this process is the observation of two-phase coexistence (e.g. water and ice) and a latent heat. The melting of 2D solids has attracted a great deal of attention over the

DISCLAIMER

past twenty five years. This activity was stimulated by the theoretical prediction of Kosterlitz and Thouless(KT)[1] which suggested that the melting of 2D solids is initiated by the unbinding of dislocation pairs. The unbinding produces a continuous melting transition in which a bond-directionally ordered liquid forms first and then evolves at higher temperatures into an isotropic liquid phase. Numerous investigations of the melting properties of solid physisorbed films were undertaken, but it is unclear whether these systems were governed by this unusual KT melting process[2]. In fact only limited evidence has been recovered which suggests that a bond-directional ordering actually forms in these systems. The ethylene on graphite system is one a the few physisorbed systems which has been found to have a heat capacity signature indicative of a continuous transition[3].

Much is known about the ethylene-on-graphite system in terms of both the structure and dynamics in the region around the melting transition. Furthermore, a systematic attempt was made to understand the difference in the behavior of the spatial and dynamical properties between ethylene and equivalent methane films since methane melting was known to be a discontinuous transition[4].

Ethylene and methane films melt from incommensurate, orientationally disordered, triangular solid structures, expanded with respect to the graphite basal plane. In both cases the melting transition proceeds from a coexisting solid-plus-vapor to a coexisting solid-plus-liquid phase. Similarly the ratio of the 2D-to-3D melting temperatures in the two cases is about 0.64 as is the ratio of the near-neighbor distance to van der Waals radii suggesting that the molecular packing in the two systems is the same. The inset to fig. 1 however, illustrates the obvious differences in the heat capacity signals recorded for each system. We note that the ethylene melting peak is about 20 times broader than the methane peak but has an area only a little more than half as large. Figs. 1 and 2 show how elastic and quasi-elastic neutron scattering methods were used to follow the temperature dependent changes in the spatial correlation range and translational diffusion in the two systems respectively. It is clear from the neutron data that the difference in the thermodynamic signatures of the melting transitions of methane and ethylene films originates from an underlying difference in the microscopic behavior which occurs in the two films. How can these differences be understood? We have previously suggested that the differences in the melting properties arises from the differences in the vacancy creation mechanisms in the two systems

For 2-D solids there are three primary mechanisms for the creation of vacancies: (i) molecules leave the periphery of the film (edge melting) (ii) molecules leave the first layer and form a partial second layer (layer promotion) or (iii) solid films composed of non-spherical molecules can create vacancies by reducing their projected area on the surface (either by a change in orientation or conformation).

Near melting, methane molecules within the solid are rotating randomly about their equilibrium position creating in-effect a spherical shape, so only vacancy creation mechanisms (i) and (ii) need to be considered. On the other hand, ethylene molecules near melting are known to sit with the plane of the molecule parallel to the graphite basal plane while executing rotational motions primarily about an axis perpendicular to the plane of the molecule[5] (creating a disk-like shape). Thus a vacancy can be created by having some molecules flip up out of the surface plane (mechanism (iii)) thereby inducing the onset of translational diffusion. Such a form of molecular "flipping" can occur without the breaking of surface bonds and could be responsible for the continuous nature of the melting transition and has been observed in computer simulations by Moller and Klein[6].

A growing body of evidence underlining the importance of the (iii) type of vacancy creation mechanism has been recently gathered by Taub and coworkers[7,8] from neutron diffraction investigations of the structures and melting properties of long chain molecules, primarily the alkanes, adsorbed on graphite.

Argon Layer-by-Layer Melting

While much work has been geared toward understanding the unusual melting properties of the 2D systems described above, a detailed understanding of the melting of 3D matter is still far from being realized. Recently there has been a considerable effort to understand the role played by the outer most layers ("the surface") of a 3D solid in the melting transition. Evidence of "surface melting" or atomic mobility in surface layers of solids at temperatures below the bulk melting point has been reported for sometime[9]. Neutron scattering techniques were used to characterize the melting properties of multilayer films of argon on graphite in an attempt to gain a deeper microscopic understanding of the role played by the outermost layers of a substance near melting. Fig. 3 illustrates how neutron techniques can be used to study the onset and layer-by-layer(LBL) melting in a three layer argon film on graphite[10,11]. Notice the stepwise increase in the integrated intensity ("window scan") at the low-Q side of the first order Bragg peak. This behavior has been shown to be consistent with LBL melting which proceeds from the layer furthest from the substrate inward. Additional elastic diffraction evidence indicates that at the plateaus are regions where the liquid layer(s) coexist with solid layers. The interaction of the argon liquid layers farthest from the graphite substrate are responsible for stabilizing the solid layer closest to the substrate which is found to melt at more than 10K above the bulk argon melting temperature of 83.8 K. Fig. 4 shows the how inelastic neutron scattering techniques can be used to track the temperature dependence of of the dynamical response of a trilayer argon film on graphite. Notice that the quasielastic signals begin to show up at temperatures above 65K. This is precisely in the same temperature range where an increase in the "window scan" intensity shows up. Further evidence of the how the solid/liquid properties of the film change with temperature can be gathered by examining how the intensity of the quasielastic signals increase while the solid "phonon" contribution to the inelastic signals near neutron energy transfers of ~2 meV move and decrease with increasing temperature. Only after the temperature increases above ~95K does evidence of the a solid film contribution disappear. A combination of elastic and inelastic diffraction, computer simulation and thermodynamic data are used to show that melting in the multilayer rare gas systems on graphite appear to occur in a LBL fashion proceeding from the surface of the film toward the substrate. Furthermore computer simulations indicate that the melting is driven by layer promotion , which is the primary vacancy creation mechanism[12-14].

Tunnelling of Methane on MgO

High-resolution INS techniques can also be used to study the rotational motions of hydrocarbon films adsorbed on solid surfaces. Pioneering work by Smalley *et al* .[15] on the rotational tunnelling properties of methane on graphite shows that INS can be used to derive information relating to the intermolecular potentials. In fact it is often stated that tunnelling measurements are the most accurate way to characterize the interatomic potentials of solid systems. The reader is directed to work by Press [16] for details concerning rotational tunnelling spectroscopy with neutrons.

Here we describe the application of INS techniques to the study of the low temperature rotational tunnelling of methane molecules on MgO(100) surfaces. MgO(100) surfaces offer an interesting alternative to the sixfold symmetry common to graphite and most close-packed metal surfaces. Elastic neutron diffraction indicates that monolayer methane forms a $\sqrt{2}X\sqrt{2}$ R45° commensurate, square-solid structure on MgO[17]. Unfortunately on the basis of elastic diffraction alone it is not possible to determine the orientation of the methane molecule. On the other hand, the behavior of rotational ground state splittings of a tetrahedral molecule in fields of different symmetry is known. It is of particular interest to focus one's attention on how the splitting of the triply degenerate T state behaves as a function of different crystal site symmetry (shown in Fig. 5). Since the solid II form of bulk methane falls in the space group Fm3c with 6 sublattices of ordered molecules with 6 sublattices with $\bar{4}2m$ site symmetry, the degeneracy of the "T" state is not raised and only two transitions should be observable. Fig. 6(a) shows the INS spectrum recorded by Asmussen *et al* .[18] for solid methane at 1.5 K. Here the two rotational tunnelling lines are clearly visible near 70μeV and 140 μeV. There is also another feature which appears in the spectrum near 1.2 meV. This is the 0->1 transition of the free rotator state of the methane molecule. A detailed explanation of this spectrum can be found elsewhere (see ref.16 and refs. therein). Equivalent results for monolayer methane on graphite are shown in fig. 6(b). While some additional fine structure is present, the tunnelling spectra from the monolayer film, like the spectra from the bulk solid, has two prominent lines. A detailed explanation can be found in a recent article by Inaba *et al* .[19].

As mention above one of the objectives of our INS investigations was to determine if something more could be learned about the orientation of methane molecules in the monolayer solid formed on MgO surfaces. Fig. 6(c) shows the tunnelling spectrum of monolayer CH_4-on-MgO. It is evident that the spectrum is different from that of either bulk CH_4 or the CH_4-on-graphite monolayer. Detailed analysis of the CH_4-on-MgO spectrum has been reported by Larese et al.[20] using data obtained earlier using poorer quality MgO powders. The analysis (following procedures outlined by Smith [20]) shows that the degeneracy of the "T" state is removed by potentials with C_{2v} symmetry. This suggests that the molecules sit in a dipod-down configuration with the C_{2v} axis of the molecule normal to the MgO surface plane. Table 1 lists the predicted positions of the various tunnelling transitions together with the experimental values obtained from the data of Fig. 6(c). Agreement is excellent. By applying symmetry arguments to tunnelling data we were thus able to determine the orientation of the molecules in the low temperature monolayer solid.

Work in progress is aimed at using the new high resolution data (Fig.6(c)) to obtain accurate values for the linewidths and intensities of the various transitions to determine the transition probabilities. Some effort has been devoted to exploring the temperature dependence of the tunnelling spectra. On heating (from 1.5K) the monolayer tunnelling spectrum is observed to broaden gradually until at temperatures above 15K it becomes a single, broad quasielastic line centered at zero energy transfer. This suggests the onset of some form of molecular rotational diffusion.

Beyond understanding the rotational tunnelling properties of the monolayer methane films lies an interesting question: Can rotational tunnelling be used to observe the crossover from 2D-to-3D [22]? In other words, does the tunnelling spectrum for monolayer CH_4 -on-MgO develop into a bulk-like CH_4 spectrum as the layer thickness increases? Adsorption isotherm and elastic diffraction measurements indicate that methane films grow in a layer-by-layer fashion on MgO(100)[23]. Furthermore, the spectra in Figs.5(a) and (c) are distinctly different. Fig. 7 shows a sample of the recent INS data collected as a function of layer thickness[24]. Two important points are worth making. First, the spectra seem to be converging towards bulk behavior at coverages of about 5 or 6 layers. Second, inelastic transitions appear in the neighborhood of the free rotor line (near 1 meV) as soon as the layer thickness increases beyond the monolayer. Actually there appears to be three distinct transitions near 1 meV which coalesce into one as the layer thickness increases. Such behavior could be an indication of the diminished influence of the MgO substrate on molecules in the second layer and beyond. The well-defined shape of the three lines in the bilayer spectrum suggests occupation of three different adsorption sites. Efforts to make a consistent identification of these sites is underway.

Summary

We have used the examples of the melting of ethylene on graphite , the layer-by-layer melting of argon multilayers and the rotational tunnelling on MgO(100) to illustrate the variety of ways that cold neutron techniques can be applied to the study of films adsorbed on solid surfaces. In the future these types of studies will be employed to explore surface mediated chemical reactions.

Acknowledgments

It is a pleasure to recognize the many collaborators who contributed to the work described here. Many thanks to L. Passell, J.M. Hastings, C. Koehler III, Q. M. Zhang, D. E. Johnson, W. Kunnmann, J. M. Phillips, C. Carlile, D. Richter, M. Klein, W. A. Steele, M. H. W. Chan, J. G. Dash, G. Hess, H. Taub, D. Kearley, D. Martin, M. Adams, B. Asmussen and D. Smith. This research was performed under the auspices of the U.S. Department of Energy, Materials Science Division, under Contract # DE-AC02-76CH00016.

References

[1] J. M. Kosterlitz and D. J. Thouless, J. Phys. C6, 1181(1973).

[2] see e.g. K. J. Strandburg, Rev. Mod. Phys. ,161(198) and refs. therein.

[3] H. K . Kim, Q. M. Zhang and M. H. W. Chan, Phys. Rev. Lett. 56, 1579 (1986).

[4] see e.g. J. Z. Larese, L. Passell, A. Heidemann, D. Richter and J.P. Wicksted, Phys. Rev. Lett. 61, 432(1986) and refs. therein.

[5] J. Z. Larese, L. Passell and B. Ravel, Can. J. Chem. 66 633(1988).

[6] M. A. Moller and M. L. Klein,

[7] W. Herwig, J. C. Newton and H. Taub, Phys. Rev. B50, 15287(1994).

[8] W. Herwig, Z. Wu, H. Taub and F.Y. Hansen, to be published in J. Chem Phys. (1997).

[9] J. G. Dash, Contemp. Phys. 30, 89 (1989) and refs. therein.

[10] D. M. Zhu and J. G. Dash, Phys. Rev. Lett. 60, 432(1988); D. M. Zhu and J. G. Dash, Phys. Rev. B38 11673,(1988).

[11] J. Z. Larese and Q. M. Zhang, Phys. Rev. Lett. 64, 922(1990).

[12] J. M. Phillips, Phys. Lett. A147, 54 (1990).

[13] A. L. Cheng and W. A. Steele, Langmuir 5 600 (1989).

[14] J. Z. Larese, Acc. Chem. Res. 26, 353(1993).

[15] M.V. Smalley *et al.* Mol. Phys. 44, 533 (1981).

[16] W. Press, in *Single-Particle Rotations in Molecular Crystals* (Springer-Verlag, Berlin, 1981).

[17] J. P. Coulomb *et al.* Phys. Rev. Lett. 54, 1536(1985).

[18] B. Asmussen *et al.*, J. Chem. Phys. 97, 1332 (1992).

[19] A. Inaba *et al.*, Physica B213, 643 (1995).

[20] J. Z. Larese *et al.*, J. Chem. Phys. 95, 6997 (1991).

[21] D. Smith, J. Chem. Phys. 66, 4587(1997); ibid 86, 4046 (1987).

[22] J. Z. Larese *et al.*, Physica B226, 221(1995).

[23] J. M. Gay, J. Suzanne and J. P. Coulomb, Phys. Rev. B41, 11346(1990).

Figure Captions

Fig. 1 Temperature dependence of the spatial correlation range in ethylene and methane monolayer films on graphite. Arrows indicate the melting temperatures. The inset show the heat capacity profiles discussed in the text. The solid lines are drawn to guide the readers eye and have no theoretical significance (from ref. [4]).

Fig. 2 Temperature dependence of the translational diffusion in ethylene and methane monolayer films on graphite. Arrows indicate the melting temperatures. The solid lines are drawn to guide the readers eye and have no theoretical significance (from ref. [4]).

Fig. 3 Fixed Q window-scan illustrating the LBL melting of an argon trilayer film on graphite. The numerals 1,2, and 3 indicate the number of *solid* layers present at that temperature. The solid line has been added for clarity and serves only as a guide to the readers eye.

Fig. 4 Inelastic neutron difference data recorded at the Institute Laue-Langevin IN5 time of flight spectrometer. Data presented recorded at temperatures indicated for an argon film initially three layers thick. The feature near 2 meV can be associated with a zone boundary phonon mode. The onset of translational diffusion (melting) signaled by the increase in the scattered intensity near 0 energy transfer (i.e. the quasielastic scattering).

Fig. 5 Level scheme for the rotational ground state of a tetrahedral molecule in crystal sites with different symmetry (see ref [16], pg. 57 for details). Notice how the degeneracy of the T state is lifted in the lower symmetry sites. Transitions are forbidden from A-to-E states.

Fig. 6 (a) Tunnelling spectrum of bulk methane solid phase II by Asmussen *et al.* (ref. [18]). (b) Tunnelling spectrum for commensurate monolayer methane on graphite film at 1.5 K recorded by author and collaborators at IRIS at ISIS, (c) Tunnelling spectrum for commensurate $\sqrt{2}X\sqrt{2}$ R45° solid monolayer methane on MgO film at 1.5 K.

Fig. 7 Coverage dependence of the tunnelling spectrum for CH_4 on MgO(100) surfaces at 1.5 K Notice the appearance of the features near 1.0 meV for films bilayer thick and greater. The bulk spectrum for CH_4 II solid shown in fig. 6(a) is included for reference.

Table Captions

Table 1 Comparison of model calculations and experimental results for commensurate $\sqrt{2}X\sqrt{2}$ R45° solid monolayer methane on MgO film at 1.5 K shown in fig. 6(c).

Transition	Model (μeV)	Experiment (μeV)
E -> T3	61	55.5 ± 0.7
T2 -> T1	109	109.9 ± 0.5
T3 -> T2	130	139 ± 1.0
E -> T2	191	195 ± 1.0
T1 -> A	216	214 ± 1.0
T3 -> T1	Not Allowed	Not Observed
E -> T1	300	305 ± 1.0
T2 -> A	325	326 ±2
T3 -> A	455	457 ±0.5

Table 1

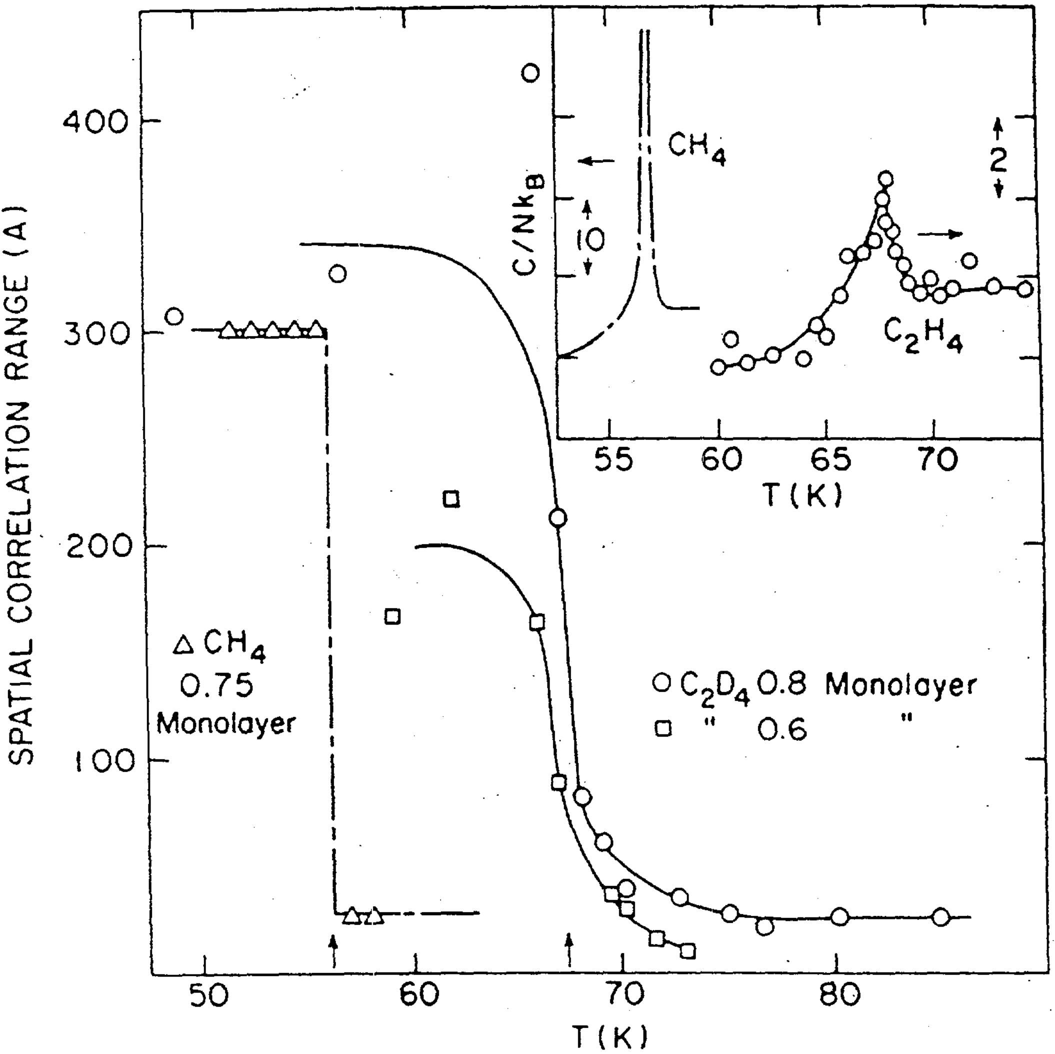
SPATIAL CORRELATION RANGE (Å)
400
300
200
100
50
60
70
80
T(K)
△ CH4 0.75 Monolayer
○ C2D4 0.8 Monolayer
□ " 0.6 "
C/Nk_B
CH4
10
2
C2H4
55
60
65
70
T(K)

JZL
FIG 1

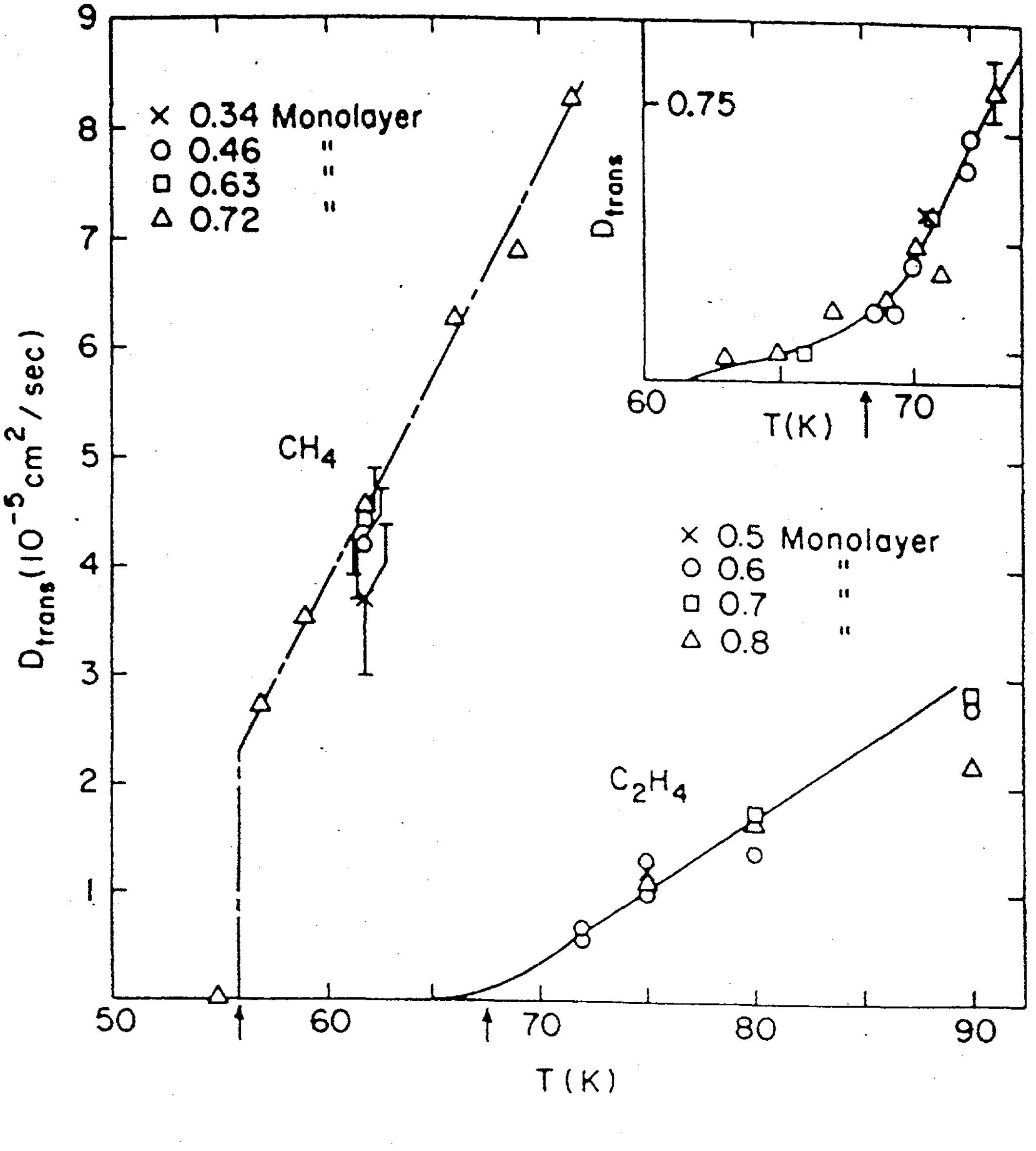
× 0.34 Monolayer
○ 0.46 "
□ 0.63 "
△ 0.72 "
CH$_4$
C$_2$H$_4$
× 0.5 Monolayer
○ 0.6 "
□ 0.7 "
△ 0.8 "
D_{trans} (10^{-5} cm^2/sec)
T (K)
50
60
70
80
90
1
2
3
4
5
6
7
8
9
0.75
D_{trans}
T(K)
60
70

JZL
FIG 2

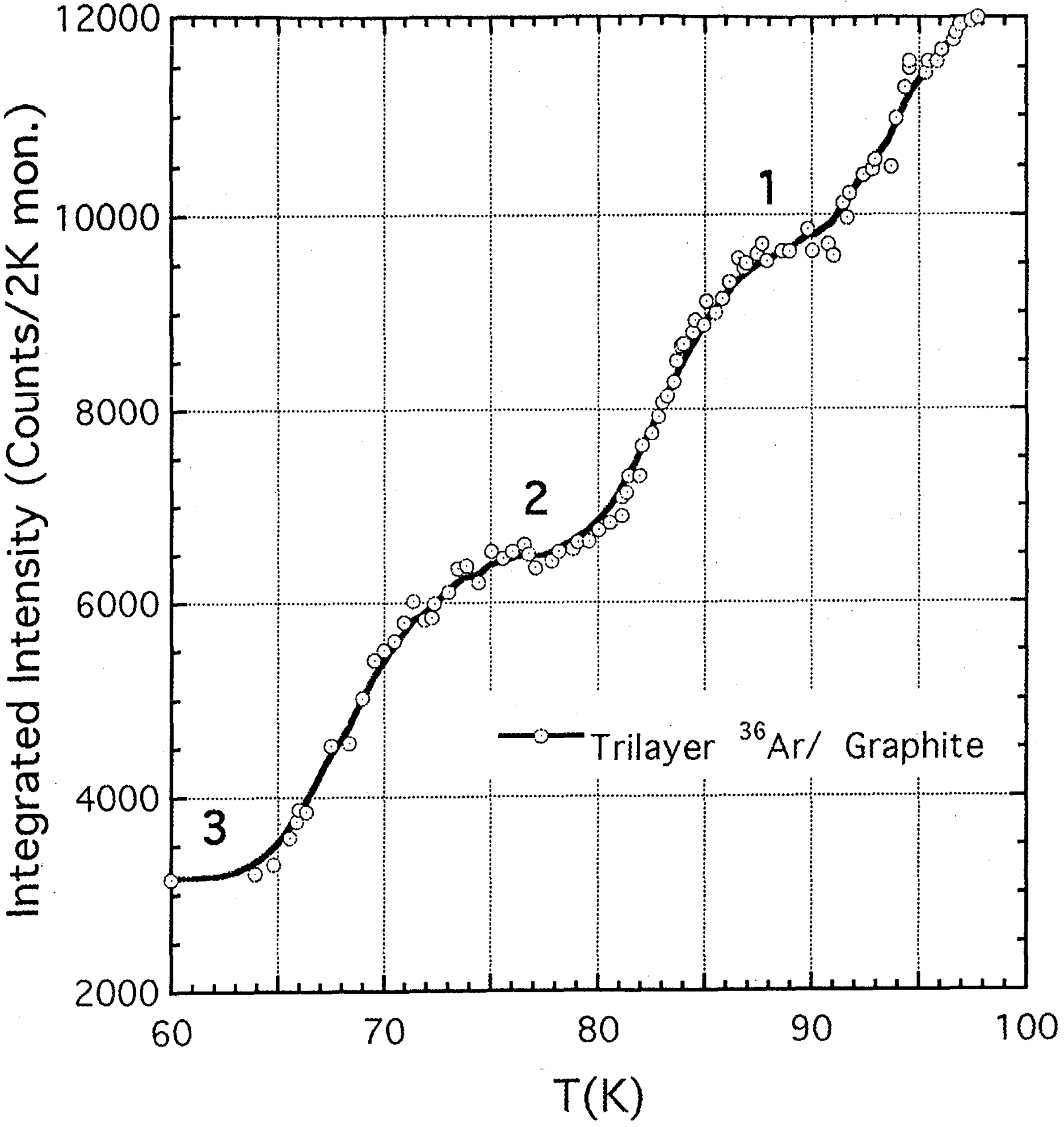

Integrated Intensity (Counts/2K mon.)
12000
10000
8000
6000
4000
2000
60
70
80
90
100
T(K)
1
2
3
Trilayer ^{36}Ar/ Graphite

JZL
Fig 8

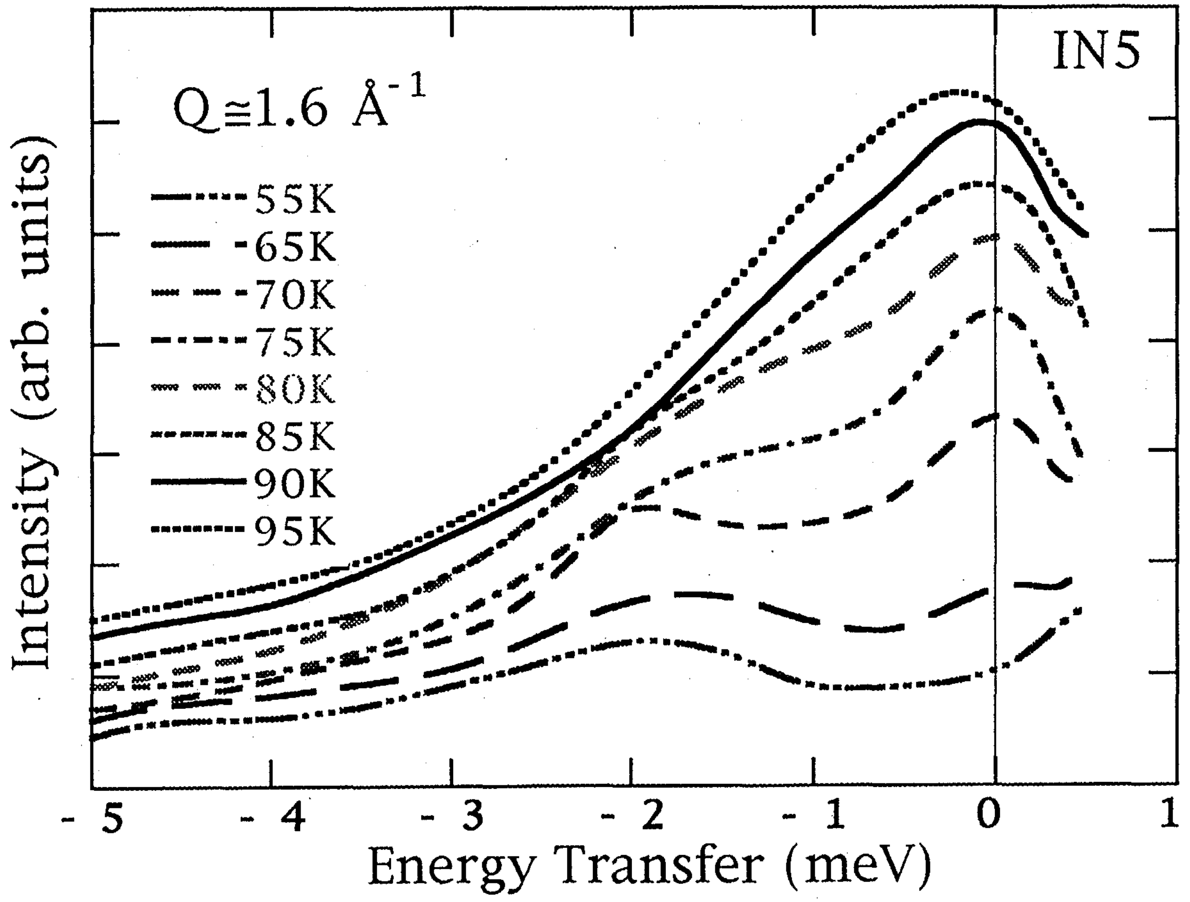
IN5
Q≅1.6 Å⁻¹
55K
65K
70K
75K
80K
85K
90K
95K
Intensity (arb. units)
- 5
- 4
- 3
- 2
- 1
0
1
Energy Transfer (meV)

JZL
Fig 4

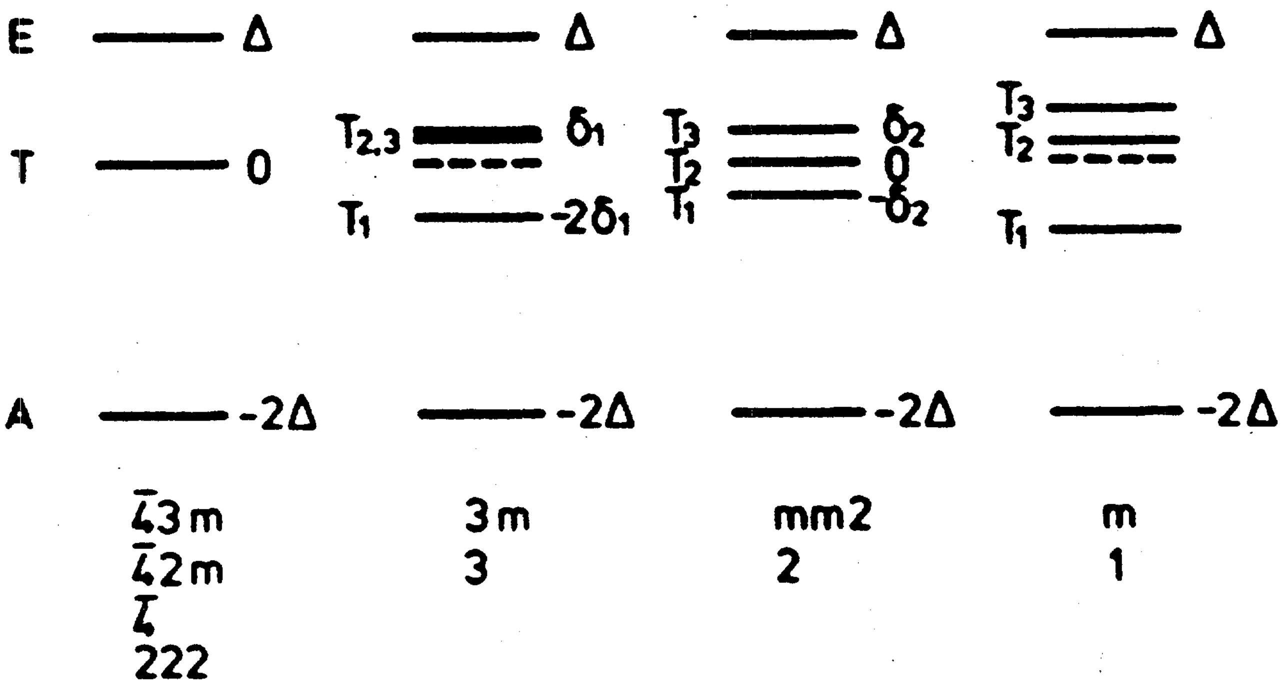
E
T
A
Δ
0
-2Δ
$T_{2,3}$
δ_1
T_1
$-2\delta_1$
T_3
δ_2
T_2
0
T_1
$-\delta_2$
T_3
T_2
T_1
$\bar{4}3m$
$\bar{4}2m$
$\bar{4}$
222
3m
3
mm2
2
m
1

JZL
FIG 5

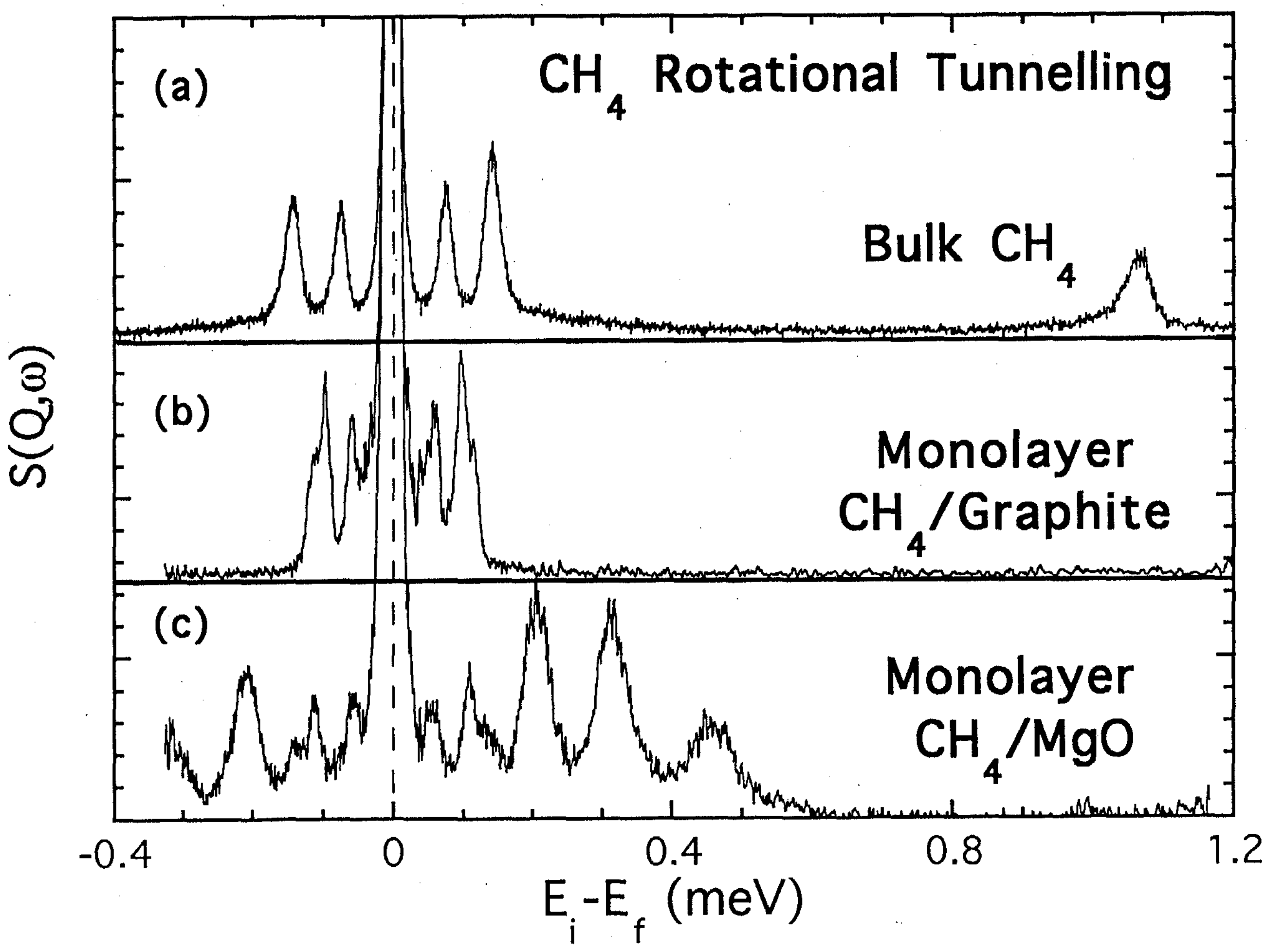
(a)
CH$_4$ Rotational Tunnelling
Bulk CH$_4$
(b)
Monolayer
CH$_4$/Graphite
(c)
Monolayer
CH$_4$/MgO
S(Q,ω)
-0.4
0
0.4
0.8
1.2
E$_i$-E$_f$ (meV)

JZL
Fig 6

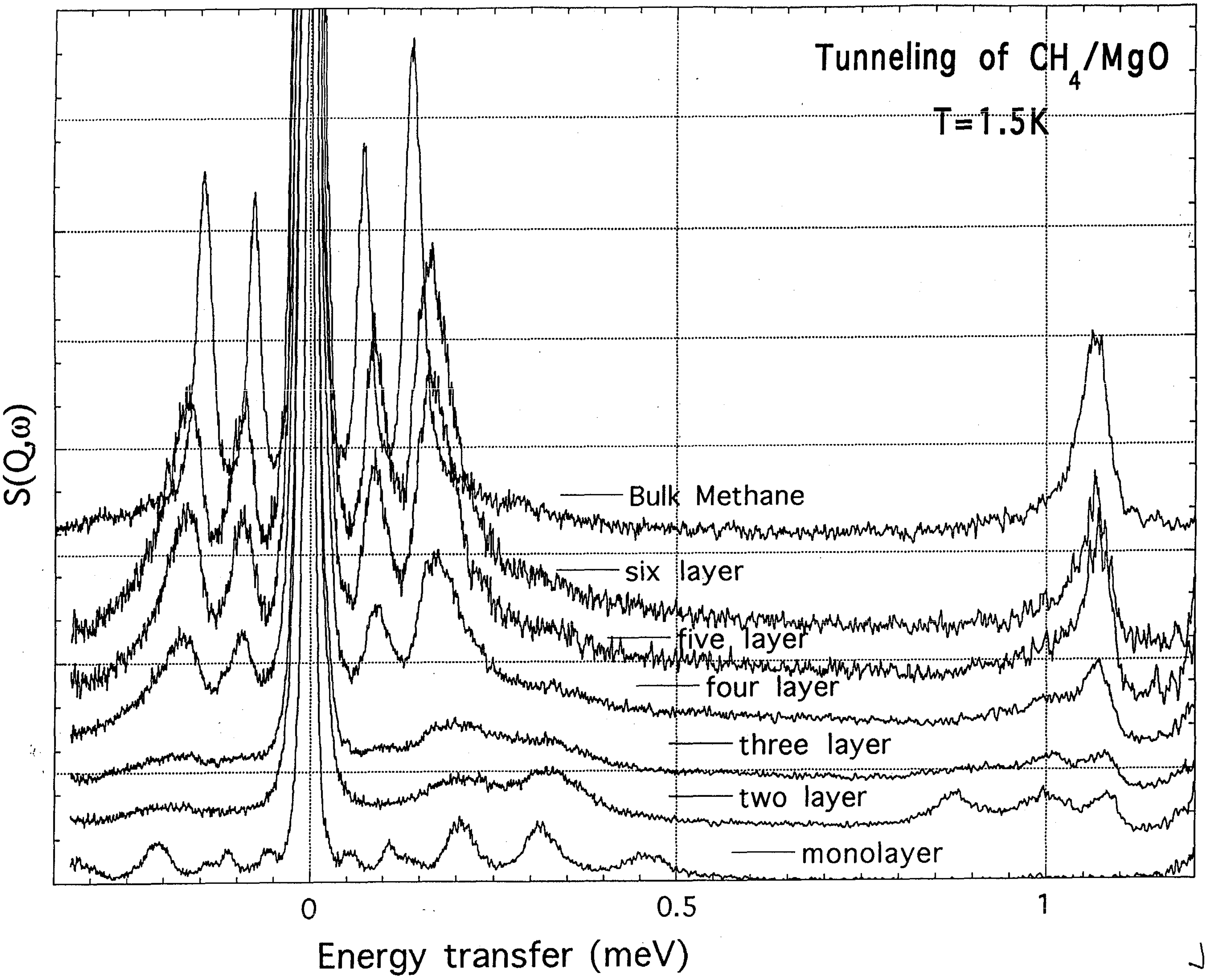
Tunneling of CH_4/MgO
T=1.5K
S(Q,ω)
Bulk Methane
six layer
five layer
four layer
three layer
two layer
monolayer
0
0.5
1
Energy transfer (meV)

J2L
Fig 7